

RESEARCH

Open Access



A nano-cocktail of the PARP inhibitor talazoparib and CDK inhibitor dinaciclib for the treatment of triple negative breast cancer

Paige Baldwin^{1†}, Shicheng Yang^{2†}, Adrienne Orriols³, Sherrie Wang³, Needa Brown^{4,5} and Srinivas Sridhar^{1,2,4,5*}

[†]Paige Baldwin and Shicheng Yang have contributed equally to this work.

*Correspondence: s.sridhar@northeastern.edu

¹ Department of Bioengineering, Northeastern University, Boston, MA, USA

² Department of Chemical Engineering, Northeastern University, Boston, MA, USA

³ Cancer Nanomedicine Co-ops for Undergraduate Research Experience (CaNCURE), Northeastern University, Boston, MA, USA

⁴ Department of Physics, Northeastern University, 360 Huntington Ave., Boston, MA 02115, USA

⁵ Department of Radiation Oncology, Brigham and Women's Hospital, Harvard Medical School, Boston, MA, USA

Abstract

Background: The addition of the cyclin dependent kinase inhibitor (CDKi) dinaciclib to Poly-(ADP-ribose) polymerase inhibitor (PARPi) therapy is a strategy to overcome resistance to PARPi in tumors that exhibit homologous recombination (HR) deficiencies as well as to expand PARPi therapy to tumors that do not exhibit HR deficiencies. However, combination therapy using pathway inhibitors has been plagued by an inability to administer doses sufficient to achieve clinical benefit due to synergistic toxicities. Here we sought to combine nanoformulations of the PARPi talazoparib, nTLZ, and the CDKi dinaciclib, nDCB, in a nano-cocktail to enhance therapeutic efficacy while maintaining lower doses.

Methods: Pharmacokinetics of nDCB were assessed to ensure it is compatible with nTLZ. nDCB was combined with nTLZ to generate a nano-cocktail nDCB:nTLZ, which elicits greater cell death in vitro compared to the combination of the free drugs. MDA-MB-231-LUC-D3H2LN xenografts were utilized to assess therapeutic efficacy of the nano-cocktail in terms of tumor progression.

Results: Administration of the nano-cocktail significantly slowed tumor progression in the HR proficient animal model compared to administration of free talazoparib and free dinaciclib at the same doses. Histology of the liver, spleen, and kidneys revealed long-term treatment did not induce nanoparticle associated morphological changes. Complete blood count did not reveal any significant hematologic changes after treatment with either the free combination or nano-cocktail.

Conclusions: The efficacy and toxicity data suggest that further dose escalation can be pursued in order to achieve a stronger response. These data suggest the administration of combination therapy through the nano-cocktail leads to a better response than the use of free compounds and is a promising strategy for implementing combination therapy in the clinic.

Keywords: Nano-cocktail, Talazoparib, Dinaciclib, PARP inhibitor, CDK inhibitor, Triple-negative breast cancer, Liposome, Micelle, Nanoparticle, Drug delivery



Background

Triple-negative breast cancer (TNBC), which lacks expression of the estrogen receptor, progesterone receptor, and human epidermal growth factor receptor 2 amplification, comprises 15–20% of all breast cancers (Li et al. 2022; Bauer et al. 2007). Although targeted therapies are becoming part of first line treatments for a number of cancers, sequential chemotherapy remains the standard of care for TNBC, due to the lack of receptor expression for targeting (Lee and Djamgoz 2018; Székely et al. 2017). Poly-(ADP-ribose) polymerase (PARP) inhibitors Olaparib and Talazoparib (TLZ) were approved in 2018 for treatment of breast cancers with defects in the homologous recombination (HR) DNA repair pathways, such as Breast Cancer Gene 1/2 (*BRCA1/2*) mutations, which have been observed in 10–20% of TNBC cases in unselected cohorts (Singh et al. 2020; Hartman et al. 2012; Gonzalez-Angulo et al. 2011). PARP inhibitors, such as TLZ, were designed as catalytic inhibitors to block the action of PARP. This hinders repair of DNA single strand breaks converting them to double strand breaks (DSBs) during replication. Tumors with mutations in their HR pathways can be targeted by repair inhibitor small molecules such as PARPi to exploit the concept of synthetic lethality resulting in irreparable DSBs and eventual cell death (Kulkarni et al. 2022; Farmer et al. 2005; Bryant et al. 2005). To date, PARP inhibitors are only approved for the treatment of advanced *BRCA*-mutant breast cancer leaving at least 80% of TNBC patients ineligible for this therapy. Given the limitations of current treatments, there is a crucial, unmet clinical need for developing innovative therapeutic strategies to broaden the use of PARP inhibitors beyond the *BRCA*-mutant subset of TNBC. This necessity emphasizes the significance of exploring novel approaches, such as the combination therapy discussed in this paper, to enhance the effectiveness of PARPi therapy and expand its applicability to other subsets of TNBC, potentially providing new avenues for patient treatment and improving clinical outcomes.

Dinaciclib (DCB), a cyclin dependent kinase (CDK) inhibitor, has been shown to ameliorate resistance to PARP inhibition through modulation of DNA repair pathways. Inhibition of CDK1 has been shown to impair the formation of *BRCA1* foci at sites of DNA damage, thus deactivating DNA damage checkpoint signaling (Johnson et al. 2009, 2011). Inhibition of either CDK9 or CDK12 has been associated with suppression of DNA damage response and repair genes; in particular, downregulation of *RAD51*, an essential component of the DNA repair complex, results in less *RAD51* foci formation at sites of DNA damage (Johnson et al. 2016; Alagpulinsa et al. 2016). DCB has also been shown to decrease expression of *MYC*, a proto-oncogene amplified in numerous types of cancer (Carey et al. 2018). *MYC* amplification increases the expression of DNA repair genes, notably *RAD51*, and these patients experience shorter time to relapse and tend to be less sensitive to PARP inhibitor treatment (Carey et al. 2018; Horiuchi et al. 2012). Therefore, DCB can downregulate a number of the key factors in HR in order to sensitize tumors with both intrinsic and acquired PARP inhibitor resistance. Preclinical studies have demonstrated that the combination of DCB with PARP inhibitors veliparib, olaparib, or niraparib can sensitize resistant models to PARP inhibition and control tumor growth (Johnson et al. 2016; Alagpulinsa et al. 2016; Carey et al. 2018). For tumors that are already sensitive to PARP inhibition, this combination has been proven to provide

a more durable response than treatment with the PARP inhibitor alone (Johnson et al. 2016; Alagpulinsa et al. 2016).

In a phase I dose-escalation study of DCB for the treatment of solid tumors, 60% of patients in all dose levels experienced grade 3–4 toxicities, with the most common being anemia, hyperbilirubinemia, neutropenia, and hypophosphatemia (Nemunaitis et al. 2013). In a phase II study investigating DCB to treat advanced breast cancer, grade 3–4 adverse events included neutropenia (47%), leukopenia (21%), increased transaminase levels (11%), and febrile neutropenia (11%). Additionally, this study was ended after 30 patients because time to disease progression was shorter for those treated with DCB compared to those treated with capecitabine (Mita et al. 2014). Pharmacokinetic assessment revealed the half-life of DCB after a 2 h infusion is 3.3 h for a dose of 58 mg/m² (Mita et al. 2017). Additional longer infusions were studied in an effort to prolong the plasma half-life but these schedules resulted in other toxicities which prevented further development of these schedules.

Preclinical studies did not demonstrate significant toxicity in animals treated with various PARP inhibitors in combination with DCB, leading to the initiation of a clinical trial to assess the combination of DCB and veliparib (Johnson et al. 2016). The recommended phase 2 dose was 30 mg/m² DCB every other week and 400 mg veliparib twice daily, however, subsequent cycles required veliparib dose reduction (Shapiro et al. 2017). Preliminary findings suggested that patients were more likely to respond when the dose of veliparib was high enough to take advantage of PARP trapping, a phenomenon in which PARP binds to the site of DNA damage and becomes “trapped,” generating a cytotoxic lesion (Shapiro et al. 2017; Murai et al. 2012). Therefore, additional arms were explored in which DCB was administered more often at a lower dose in an effort to maintain the PARP inhibitor dose. The short plasma half-life of DCB may contribute to the difficulty in combining DCB with veliparib.

Of the commercial PARP inhibitors, TLZ is the most potent PARP trapper while veliparib is the least potent (Lord and Ashworth 2017). It has been suggested veliparib is the easiest PARP inhibitor to combine with other therapies due to the lack of PARP trapping (Matulonis 2018). Even so, the combination of veliparib and DCB still resulted in dose reduction and suboptimal treatment clinically, suggesting there will be challenges combining DCB with any PARP inhibitor. We have previously developed a nanoformulation of TLZ, nTLZ, and demonstrated that the nanoformulation increases both the time to disease progression and overall survival, compared to equivalent doses of i.v. and oral TLZ in a murine model of spontaneous breast cancer (Zhang et al. 2019). Additionally, treatment with nTLZ did not induce any signs of alopecia, while both oral and i.v. TLZ did elicit this phenotype in 25% of animals. Therefore, nTLZ offers an avenue for combining PARP inhibition with other therapies, such as DCB, with the potential for less toxicity (Singh et al. 2020; Yang et al. 2021). The short half-life of DCB and incidence of adverse events suggests the combination with nTLZ will not ameliorate all of the challenges associated with DCB combination therapy (Fig. 1A) (Paige Baldwin et al. 2021). Therefore, we hypothesized that the development of a nanoformulation (nDCB) of DCB, which can extend the half-life of DCB would be better suited for combination with nTLZ. We hypothesized that the co-delivery of nTLZ and nDCB in a nano-cocktail would result in better efficacy than co-delivery of the free drugs (Fig. 1B). We further

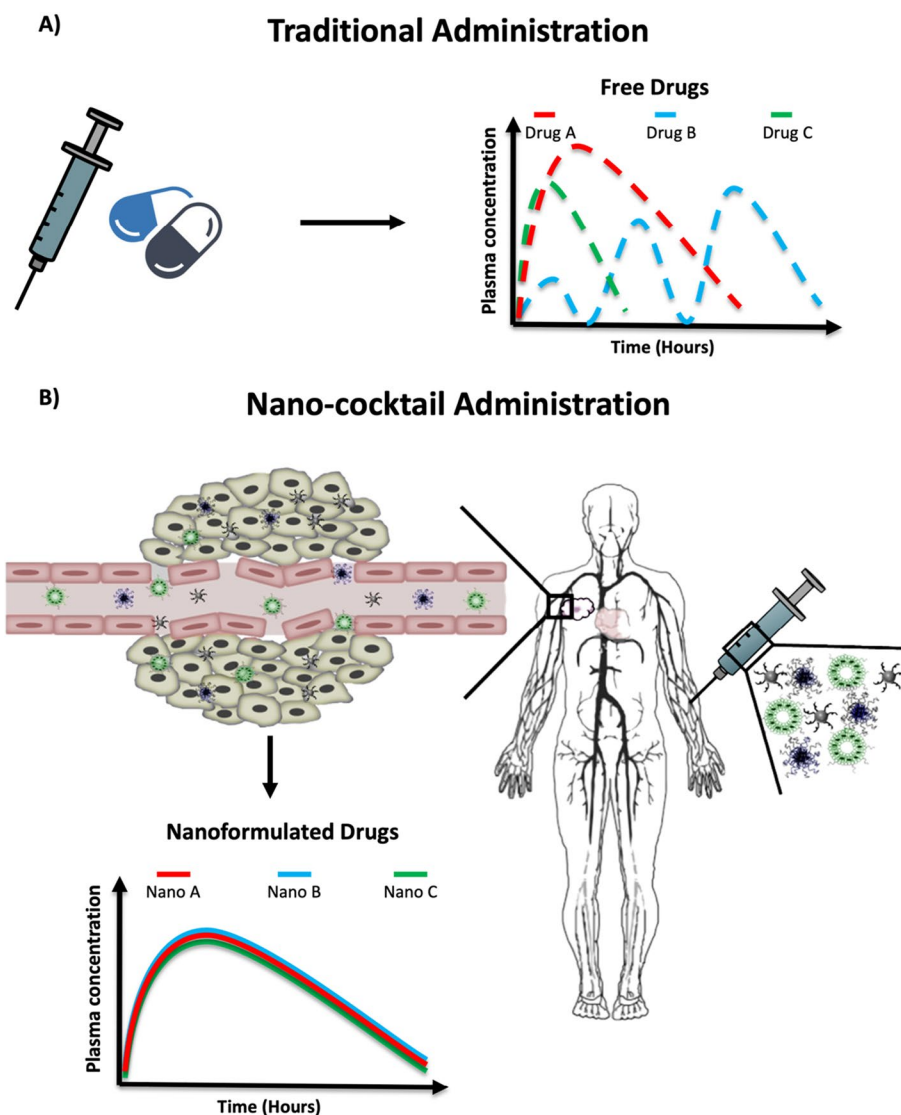


Fig. 1 **A** Traditional free drug delivery approaches limit efficacy of combinatorial strategies due to challenges associated with varying pharmacokinetics that may result in loss of synergy. Here, the short half-life of Drug A suggests the combination with Drug B and Drug C will not synergize and ameliorate all of the challenges associated with this combination therapy. **B** The co-delivery of different drugs in a nano-cocktail would result in better efficacy than co-delivery of the free drugs

hypothesized that this would reduce the toxicity of the combination by allowing for lower doses to be administered while still proving efficacious.

Here we describe nDCB, a polymeric formulation of DCB, which when administered as part of a nano-cocktail with nTLZ elicits a therapeutic effect in TNBC xenografts. nDCB extends the half-life of DCB considerably compared to the reported half-life of free DCB. An orthotopic model of TNBC was generated in mice to test the effect of nDCB:nTLZ compared to DCB:TLZ in tumors with no known defects in HR. Complete blood count was assessed for nDCB:nTLZ and DCB:TLZ to determine whether these doses elicited any hematologic toxicity. The results of this study demonstrate that nano-cocktail may be a promising strategy for combining two drugs with different

pharmacokinetics (PK) in order to produce a similar PK/PD relationship and offer therapeutic benefit at nontoxic doses.

Methods

Throughout this paper we have used the following nomenclature. DCB and TLZ stand for free drug. nDCB and nTLZ represent the corresponding nanoformulations. Mixtures are named as DCB[concentration]:TLZ[concentration] or DCB[concentration]:nTLZ[concentration]. In the dose response curve, x:y ratio of mixture are named as DCB[x]:TLZ[y] or nDCB[x]:nTLZ[y]

Synthesis of nDCB

nDCB was synthesized using Poly(D,L-lactide-co-glycolide), 50:50, acid terminated, M_w 7,000–17,000 (PLGA) and Methoxy Poly(ethylene glycol)-b-Poly(lactic-co-glycolic acid), 50:50, $M_w \sim 5000:10000$ (mPEG-PLGA) from Sigma Aldrich and PolySciTech, respectively. PLGA and mPEG-PLGA were both dissolved in acetonitrile, and the weight ratio of the two components was varied systematically from 10:0 mPEG-PLGA:PLGA to 1:9. DCB was dissolved in dimethylsulfoxide (DMSO) and added to the polymer mixture (10 wt %). Nanoparticles were formed via nanoprecipitation using the NanoAssemblr Benchtop (Nanoassemblr, Precision NanoSystems Inc., Vancouver) with deionized (DI) water as the aqueous phase. After optimizing the formulation, nDCB was synthesized using a 8:2 ratio of mPEG-PLGA:PLGA: at a total polymer concentration of 50 mg/mL. The aqueous to organic flow rate ratio was 4:1 and the total flow rate was 8 mL/minute. The organic solvent and free drug molecules were removed by washing the formulation twice at 2100 rcf for 15 min using a Macrosep Advance Centrifugal Device with a molecular weight cutoff of 100 K. After washing the formulation was resuspended using 10X phosphate buffered saline (PBS) and DI water to a final concentration of 1X PBS. Vehicle nanoparticles were synthesized in the same manner without the addition of DCB.

Formulation characterization

Size and zeta potential of the nanoparticles were measured using a Brookhaven 90Plus dynamic light scattering (DLS) analyzer equipped with ZetaPALS. Nanoparticles were diluted 1:100 in PBS for all measurements. Size was confirmed by Transmission Electron Microscopy (TEM) with a negative stain of 2.0% uranyl acetate. The concentration of encapsulated DCB was measured by lysing nanoparticles with acetonitrile prior to High Performance Liquid Chromatography (HPLC) analysis. HPLC was performed on an Agilent 1260 Infinity II with a ZORBAX 300StableBond C18 column. The mobile phase A consisted of acetonitrile with 0.1% trifluoroacetic acid, and the mobile phase B consisted of water with 0.1% trifluoroacetic acid. An isocratic elution was carried out at a ratio of 80:20 A:B. The flow rate was 1.8 mL/minute and DCB was detected with a wavelength of 254 nm at ~ 0.84 min.

The stability of nDCB in storage was measured for up to 2 months after synthesis. All formulations were stored at 4 °C. Size and zeta potential were measured 1 week, 2 weeks, 1 month, and 2 months post synthesis as described above. All studies were conducted in triplicate.

150 μL of nDCB was added to individual Thermo Scientific Slide-A-Lyzer MINI dialysis unit (10 K MWCO) and placed in a PBS bath, pH 7.4 at 37 °C, under constant stirring, to produce sink conditions. At predetermined time points (0.5, 1, 2, 4, 6, 8, 10, 24, 30 h), an aliquot of the nanoparticle solution was removed and lysed for HPLC analysis. All studies were conducted in triplicate.

nTLZ synthesis and characterization

nTLZ was synthesized and characterized as previously described (Zhang et al. 2019; Baldwin et al. 2019). Briefly, lipid nanoparticles were formed via nanoprecipitation using the NanoAssemblr Benchtop. Each batch of nTLZ was characterized in regard to size, zeta potential, and loading prior to use.

Cell culture

MDA-MB-231-LUC-D3H2LN (231) cells (provided by Zdravka Medarova, Massachusetts General Hospital, Boston, MA) and 4T1 cells (purchased from ATCC, CRL-2539TM) were cultured in DMEM with 10% FBS and 1% Pen/Strep (Corning Cellgro). All studies were conducted in triplicate. High grade serous ovarian cancer (HGSO) 3666 cells were cultured as described the previous studies (Yang et al. 2023).

231 cells were seeded into 96 well plates at 1,000 cells per well. 4T1 cells and 3666 cells were seeded into 96 well plates at 500 cells per well. The following day, cells were exposed to either DCB or nDCB at concentrations ranging from 0 to 5 μM or TLZ or nTLZ doses ranging from 0 to 10 μM . For fixed ratios of DCB:TLZ the DCB and nDCB concentrations ranged from 0 to 50 nM. Therefore, the TLZ and nTLZ concentrations ranged from 0 to 50 nM, 0–150 nM, or 0–500 nM for 1:1, 1:3, and 1:10, respectively. For fixed concentrations of combination treatment, cells were exposed to either 0–500 nM of DCB or nDCB in the presence of 10 nM TLZ or nTLZ, or exposed to either 0–500 nM of TLZ or nTLZ in the presence of 10 nM or 25 nM of DCB or nDCB. One week after seeding, cell viability was ascertained by the MTS assay to measure the metabolic activity of the cells. Data from dose response experiments were plotted and fit using a variable slope four-parameter logistic equation constrained at 100 and 0. Combination indices were calculated using Compusyn (Chou 2005).

Long-term viability at a ratio of DCB[1 nM]:TLZ[10 nM] was assessed using two different dosing regimens. 1,000 cells were seeded into 12 well plates. The following day, cells were treated with doses of 10 nM TLZ and 1 nM DCB. Equivalent dosing was used for nTLZ and nDCB treatment. After 6 days of treatment, the media was replaced, and cells were allowed to grow drug-free for an additional 7 days. In an alternative scheme, cells were treated sequentially with either 1 nM DCB or nDCB for 3 days, followed by a 3 day treatment with either 10 nM TLZ or nTLZ. After the treatment period, the media was replaced, and cells grew drug-free for 7 days. Cells were then fixed with formalin and stained with crystal violet. To quantify the cell growth, the crystal violet was solubilized with 5% acetic acid under gentle shaking, and the absorbance was measured at 563 nm.

Pharmacokinetics

All animal studies were performed in accordance with protocols approved by the Institutional Animal Care and Use Committee at Northeastern University. An orthotopic xenograft model of human TNBC was established via injection of 1×10^6 MDA-MB-231-LUC-D3H2LN cells (cultured in DMEM with 10% FBS and 1% Pen/Strep) in 50% matrigel (Corning) and into the mammary fat pad of female NCr-nu/nu mice (Charles River Laboratory).

Mice with tumors $\sim 100 \text{ mm}^3$ in size were administered a single dose of 1 mg/kg i.v. nDCB. Mice were euthanized at designated time points (0.083, 0.5, 1, 6, and 24 h) after treatment for sample collection ($n=5/\text{group}$). Blood was collected via cardiac puncture into K2 EDTA microtainers. Blood was centrifuged at 1,600 g for 15 min at 4 °C. Plasma was separated and frozen at -80 °C until processed. Acetonitrile was added to precipitate plasma proteins. Samples were centrifuged at 14,000 g for 5 min, and the supernatant was filtered with a 0.2 μm syringe filter. Each sample was dried overnight and reconstituted in 200 μl of acetonitrile for analysis via HPLC. HPLC conditions were as detailed above. A standard curve was prepared by processing plasma from untreated animals and spiking the samples with known amounts of DCB when reconstituting the samples. A non-compartmental analysis was fit using PKSolver (Zhang et al. 2010).

In vivo efficacy

The therapeutic efficacy of the combination of nDCB:nTLZ was assessed in orthotopic 231 xenografts. 1×10^6 cells in 50% matrigel (Corning) were implanted in the mammary fat pad of female NCr-nu/nu mice. When tumors reached between 50 and 100 mm^3 , mice were randomized into 8 groups: no treatment ($n=6$), vehicle ($n=6$), TLZ ($n=6$), DCB ($n=6$), DCB:TLZ ($n=10$), nTLZ ($n=6$), nDCB ($n=6$), and nDCB:nTLZ ($n=10$). In vivo treatments were administered i.v. at a dose of 0.33 mg/kg for TLZ formulations and 1.0 mg/kg for DCB formulations. Vehicle treatments were the volume equivalent of each empty nanoparticle, to match the treatment of the combination nanotherapy group. Animals were treated every other day until tumors reached 1000 mm^3 . Animals were weighed and tumors measured using calipers during each treatment. Tumor volume was calculated using the following formula: $V = 0.5 \times L \times W^2$, where L was the longest dimension and W was the dimension perpendicular to L.

Histology

Liver, kidneys, and spleen were harvested during necropsy and fixed in 10% formalin. Harvested tissues were embedded in paraffin, cut, and stained by the Dana-Farber/Harvard Cancer Center Research Pathology Core. Slices of the organs were stained with hematoxylin and eosin (H&E).

Toxicity

Mice bearing 231 tumors were treated with either 3 doses of empty nanoparticles ($n=3$), DCB:TLZ ($n=4$), or nDCB:nTLZ ($n=4$). 24 h after the final treatment animals

were euthanized and blood collected via cardiac puncture into K2 EDTA microtainers. All samples were immediately sent to VRL labs for complete blood count.

Statistical analysis

All in vitro data were plotted as mean \pm SD. The statistical significance of in vitro data was determined by using Student's t-tests with $\alpha=0.05$ for significance. All in vivo data were plotted as mean \pm SEM. Normality of all data was tested with the D'Agostino-Pearson test and $p < 0.05$ not considered a normal distribution. All data followed a normal distribution and significance was tested with one-way ANOVA followed by Tukey's test for significance with $\alpha=0.05$. The log-rank test with the Bonferroni correction for multiple comparisons was used to assess family-wise significance of survival curves. Log(inhibitor) vs. response curve with best fit IC_{50} values and Kaplan Meier survival curves were generated by GraphPad Version 9.5.1.

Results

nDCB characterization

PLGA and mPEG-PLGA were utilized to create a polymeric nanoparticle in which DCB was embedded within the PLGA core. Rapid optimization was conducted using a controlled nanoprecipitation reaction in a microfluidic device. The only parameters varied initially were the ratios of PLGA and mPEG-PLGA polymers. As expected, formulations with higher concentrations of PLGA led to a larger mean diameter, suggesting a larger polymer core. As the concentration of PLGA surpassed that of mPEG-PLGA, a secondary population of larger particles was detected and at a ratio of 1:9 the polymers precipitated. These large particles are indicative of insufficient stabilization, yielding polymer aggregates. Based on size and encapsulation,

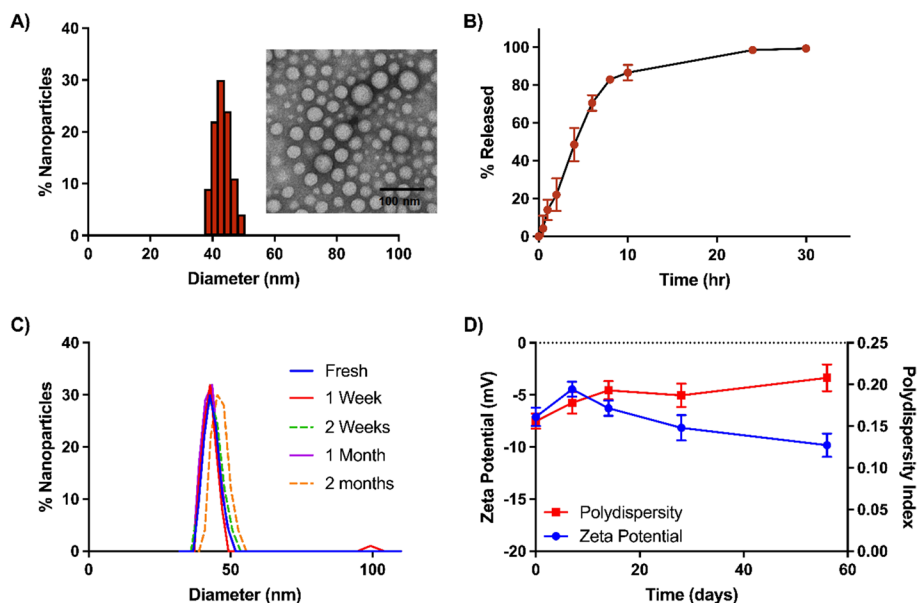


Fig. 2 Characterization of nDCB via **A** DLS and (inset) TEM reveals particles of 45 nm in diameter. Release kinetics **B** at 37 °C under constant agitation demonstrates sustained release. Size **C**, zeta potential and polydispersity index (PDI) **D** remain stable over the course of 2 months stored at 4 °C

a ratio of 8:2 mPEG-PLGA was chosen for further optimization. DLS revealed the hydrodynamic diameter of nDCB to be 46.1 ± 3.8 nm, while TEM confirmed this size distribution (Fig. 2A). nDCB was found to release fully over the course of 30 h, with ~80% of the drug releasing within the first 8–10 h (Fig. 2B). Size, polydispersity, and zeta potential measurements over time revealed the formulation remained stable in physicochemical properties over the course of 2 months in storage at 4 °C (Fig. 2C, D).

nDCB synergizes with nTLZ in vitro

Dose response was conducted on DCB and nDCB to assess whether the nanoformulation was as effective as the free drug on human TNBC, BRCA-proficient MDA-MB-231-LUC-D3H2LN cells. nDCB was significantly more potent in vitro with an IC_{50} of 5.6 ± 0.8 nM compared to 10.7 ± 0.8 nM for DCB (Fig. 3A, $**p < 0.01$). Next, we wanted to assess the potency of the nDCB:nTLZ combination. For MDA-MB-231-LUC-D3H2LN cells, as the TLZ concentration increased from 1:1 to 1:3 to 1:10 (DCB:TLZ) cell viability decreased. At all ratios the viability of cells treated with nDCB:nTLZ was lower than that of cells treated with the equivalent doses of DCB:TLZ (Fig. 3B). The combination indices (CI) indicated all ratios were synergistic, with 1:1 for both free drugs and nanoformulations exhibiting the least synergism (Fig. 3C).

A long-term growth assay was conducted with the nDCB[1 nM]:nTLZ[10 nM] treatment in order to determine the optimal dosing strategy for the combination. It was found monotherapy treatment with DCB or nDCB and TLZ or nTLZ treatment yielded insignificant growth inhibition compared to DMSO or nanoparticle vehicles, respectively (Fig. 3D). Treatment with DCB[1 nM]:TLZ[10 nM] concurrently resulted in $26 \pm 3\%$ viability compared to DMSO controls while treatment with nDCB[1 nM]:nTLZ[10 nM] concurrently resulted in $16 \pm 5\%$ viability compared to nanoparticle vehicle controls (Fig. 3D, E). In accordance with the dose response assays the combination of nDCB[1 nM]:nTLZ[10 nM] resulted in significantly lower viability compared to the combination of the free drugs ($*p < 0.05$).

In order to ensure DCB efficiently sensitized 231 cells to TLZ, the TLZ dose response assay was conducted in combination with 10 nM DCB. The addition of 10 nM DCB shifted the IC_{50} value of TLZ from 56.3 ± 18.8 nM to 23.0 ± 6.6 nM (Fig. 3F, *, $p < 0.05$). Similar results for fixed concentration or fixed ratio combination treatments of free drug, in which the IC_{50} s significantly decreased compared to their corresponding monotreatments (Additional file 1: Figure S1A) was seen in an additional murine model of BRCA-deficient metastatic ovarian cancer 3666 cells. The addition of 10 nM TLZ shifted the IC_{50} value of DCB from 11.7 ± 0.5 nM to 8.1 ± 1.57 nM, and the addition of 25 nM DCB shifted the IC_{50} value of TLZ from 6.2 ± 0.3 nM to 3.5 ± 0.2 nM. The DCB:TLZ treatment showed a IC_{50} of 3.6 ± 1.1 nM, which is significantly lower than the monotreatments. Additionally we studied the impact of the combination treatment on a BRCA-proficient murine model of TNBC4T1 cell line, in which the addition of 25 nM nDCB shifted the IC_{50} value of nTLZ from 60.9 ± 9.7 nM to 12.2 ± 9.4 nM (Fig. 3G, Additional file 1: Figure S1B).

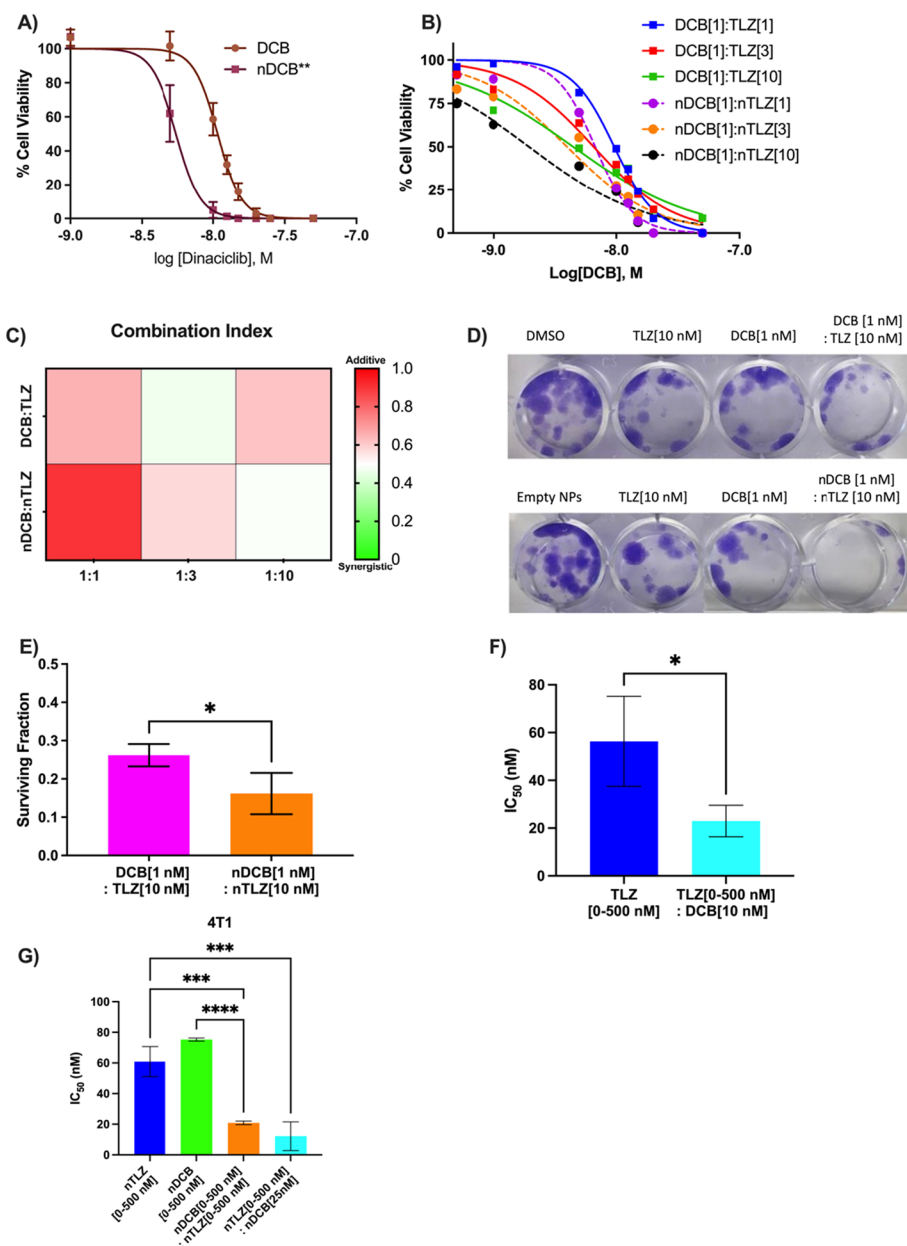


Fig. 3 nDCB is more potent than DCB **A** in a human BRCA-proficient TNBC MDA-MB-231-LUC-D3H2LN model. Dose response for the 231 cell line of the combination treatment at three different ratios **(B)** and corresponding combination indices **(C)** for each ratio. Representative images of **(D)** treatments has been presented and survival fraction has been quantification **(E)**. Prior treatment with DCB sensitizes 231 cells to TLZ **(F)** as evidenced by a shift in the IC₅₀ value. Calculated IC₅₀ of **(G)** 4T1 cell line, a murine BRCA-proficient metastatic, TNBC model, and best fit IC₅₀ values were generated by GraphPad Version 9.5.1 from Log(inhibitor) vs. response curve. *p < 0.05, **p < 0.01, ***p < 0.001, ****p < 0.0001

Combination treatment in vivo efficacy

Pharmacokinetics of nDCB were assessed after a single 1 mg/kg dose was administered (i.v.) to mice bearing 231 xenografts. Plasma was collected and DCB was extracted for HPLC analysis. The plasma data was assessed using non-compartmental analysis, the linear trapezoidal rule, and the half-life was determined to be 30.7 h (Fig. 4A).

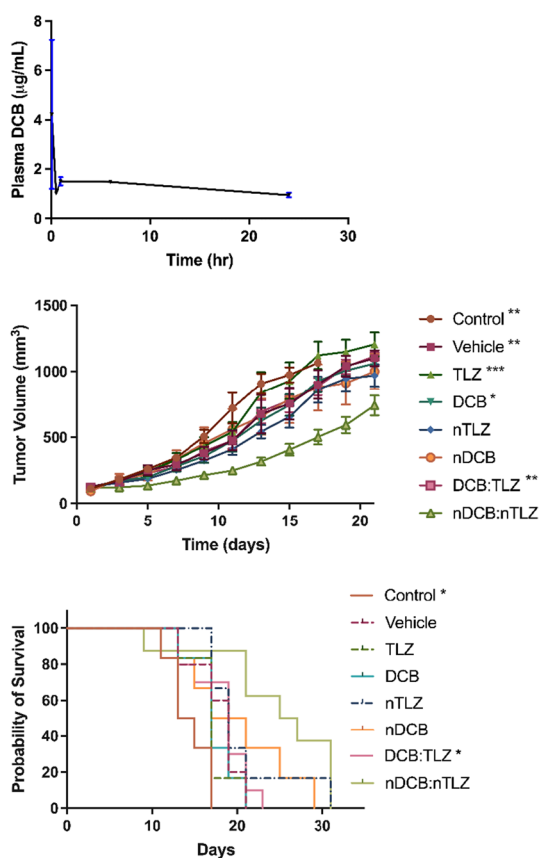


Fig. 4 **A** Pharmacokinetics was calculated using PKSolver non-compartmental analysis software and demonstrated nDCB is long-circulating. **B** Tumor volume over time represents disease progression for up to 19 days; * $p < 0.05$; ** $p < 0.01$; *** $p < 0.001$ vs. nDCB:nTLZ. **C** Overall survival demonstrated nDCB:nTLZ extends survival; * $p < 0.05$ vs. nDCB:nTLZ

Mice bearing 231 xenografts were treated with either 0.33 mg/kg TLZ or nTLZ (i.v.) or 1.0 mg/kg DCB or nDCB (i.v.) every other day. Combination treatments, DCB:TLZ or nano-cocktail nDCB:nTLZ, were administered on the same schedule with the same dosing. The vehicle group consisted of a volume equivalent to the nTLZ carrier and the nDCB carrier system. Untreated tumors grew exponentially, resulting in a mean survival of 14.3 ± 2.4 days for the control animals. While the various treatments slowed tumor growth compared to the controls, nDCB:nTLZ was the only treatment to have a significant effect. After 3 weeks of treatment, day 19, the tumor volume was significantly lower for mice treated with nDCB:nTLZ, compared to both control groups (** $p < 0.01$), both free drug monotherapies (* $p < 0.05$ vs. DCB and *** $p < 0.001$ vs. TLZ), and the free drug combination therapy (** $p < 0.01$) (Fig. 4B). The relative tumor volume as assessed by fold change was significantly lower for the nano-cocktail nDCB:nTLZ, 5.3 ± 0.6 , compared to the DCB:TLZ, 8.9 ± 0.4 (* $p < 0.05$). Although nano-cocktail nDCB:nTLZ did not induce regression, it did extend survival time compared to the free combination, with a median survival time of 26 days vs. 19 days (Fig. 4C, * $p < 0.05$). Additional file 1: Figure S2 presents individual graphs of tumor volume over time and overall survival for additional visualization.

nDCB:nTLZ is well tolerated

Body weight was measured daily and on average no significant weight loss was observed (Additional file 1: Figure S3). One animal in the nano-cocktail nDCB:nTLZ group did experience a 20% loss in body weight 7 days after treatment initiation, and was euthanized. To assess potential hematologic toxicities after treatment animals were treated with 3 doses of either DCB:TLZ or nDCB:nTLZ. 24 h after the final dose blood was collected and complete blood count assessed white blood cell (WBC), red blood cell (RBC) and platelet (PLT) counts. Neither of the combination drug treatments resulted in a significant difference in WBC, RBC, or PLT counts compared to vehicle (Fig. 5A–C). At the endpoint livers, kidneys, and spleens were collected from animals in all groups to assess nanoparticle related toxicity. H&E staining revealed no significant morphological changes in these tissues (Fig. 5D).

Discussion

A nanoformulation of DCB was synthesized in an effort to enhance efficacy while reducing toxicity such that the nanoformulation could be utilized with a previously developed nanoformulation of TLZ. In vitro assessment of the combination demonstrated DCB:TLZ and nDCB:nTLZ were synergistic at 3 different ratios, suggesting a viable combination. The in vitro IC₅₀ data suggests synergy of this combination treatment not only for BRCA mutant ovarian cancer cell line, but also for BRCA wild type breast cancer cell lines. A long-term growth assay was conducted in order to determine the optimal dosing strategy for the combination. Parry et al. demonstrated the effect of DCB can persist for hours after treatment and that continuous exposure may not be necessary for activity (Parry et al. 2010). Therefore, we assessed whether it would be appropriate to

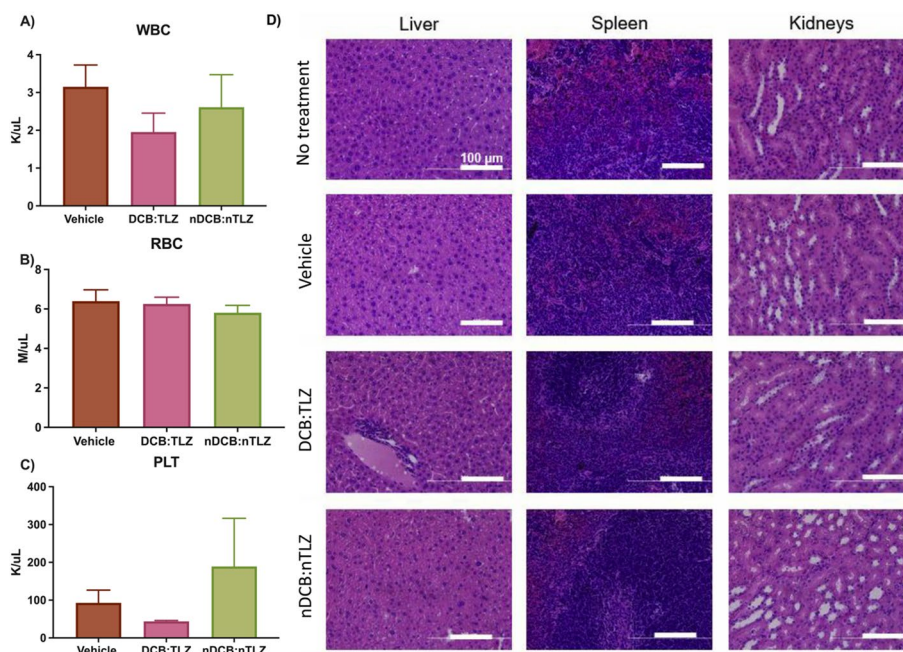


Fig. 5 Hematologic toxicity of DCB:TLZ and nano-cocktail nDCB:nTLZ assessed by **A** WBC, **B** RBC, and **C** PLT count. Representative slices of kidneys, livers, and spleens **D** stained with H&E demonstrate no gross morphological organ damage

pretreat with DCB to disrupt HR prior to treatment with TLZ. The sequential treatment with DCB or nDCB followed by TLZ and nTLZ was not found to be advantageous in regard to cell growth *in vitro*. In contrast, the simultaneous treatment with both compounds was extremely effective. This is likely because TLZ induced genomic instability relies on an accumulation of DNA damage through a number of replication cycles and therefore more time is necessary to capture TLZ induced DNA damage.

The benefit the nano-cocktail nDCB:nTLZ offered by slowing tumor progression and extending survival time was likely due to the modified pharmacokinetics of nDCB and nTLZ. The plasma drug levels of nDCB indicated a half-life of 30.7 h, in contrast the half-life of DCB administered intraperitoneally (*i.p.*) has been reported to be 0.25 h, suggesting the nanoparticle potentially altered the pharmacokinetics of the compound (Parry et al. 2010). It is important to note differences in the experimental design in that the reported half-life of DCB was after an *i.p.* administration of 5 mg/kg DCB and our study assessed a 1 mg/kg *i.v.* injection of nDCB, meaning these half-lives are not directly comparable. However, it is worth noting that in humans, free dinaciclib has a reported half-life of 2–3 h following a 2 h *i.v.* infusion, which is still significantly shorter than the nDCB formulation presented here (Mita et al. 2017). The overlapping pharmacokinetic profiles indicated nDCB and nTLZ should work in concert with one another if administered as a nano-cocktail nDCB:nTLZ, and it is expected this was the reason therapeutic benefit was observed with nDCB:nTLZ and not DCB:TLZ.

Johnson et al. demonstrated the utility of DCB with the PARP inhibitors olaparib and veliparib in models that were both PARP inhibitor sensitive and resistant (Johnson et al. 2016). Treatment after 154 days with 30 mg/kg DCB 2 × weekly and 50 mg/kg veliparib 2 × daily was not found to induce end-organ toxicity, suggesting the combination is tolerable. However, as the combination of veliparib and DCB progressed into a phase I clinical trial tolerable doses were achieved, but overall patient responses were modest, and additional tolerable dosing regimens were to be pursued (Shapiro et al. 2017). In a phase III clinical trial 52% of patients treated with oral TLZ presented with anemia, low RBC count, 27% thrombocytopenia, low PLT count, and 17% leukopenia, low WBC count (Litton et al. 2018). Only 3% of patients treated with DCB presented with thrombocytopenia (Mita et al. 2017). Neutropenia, a depletion of a subset of WBCs, is common between both drugs, with 35% of patients treated with TLZ and 43% treated with DCB experiencing this condition. After 3 doses of DCB:TLZ or nDCB:nTLZ, no significant differences in any of the blood cell counts were observed with either combination compared to vehicle, though the WBC and PLT counts for the free combination were slightly lower. This data demonstrates that at the doses utilized in this study, these side effects have not yet manifested. Additionally, the histology indicated no nanoparticle or drug induced morphological changes to the kidneys, liver, or spleens.

The therapeutic benefit offered by the nano-cocktail nDCB:nTLZ compared to the cocktail DCB:TLZ combined with a lack of observed toxicity provides a rationale for dose-escalation. This study presents proof-of-concept that a nano-cocktail composed of two formulations with similar pharmacodynamics (PD) profiles can be used to rationally administer combination therapies. The efficacy data combined with a lack of observed hematologic toxicity or organ related toxicity suggests dose-escalation is a viable next step to achieve disease stabilization or regression.

Conclusion

A nanoformulation of DCB was optimized such that it could effectively be combined with nTLZ for combination PARPi:CDKi treatment. Encapsulation of DCB in a polymeric core modified the PK/PD profiles to be more compatible with nTLZ and allowing for administration as a nano-cocktail. The nano-cocktail nDCB:nTLZ slowed the growth of HR-proficient TNBC xenografts significantly compared to the combination of DCB:TLZ. There was no observed hematologic toxicities with the doses utilized. While the combination did not arrest tumor growth, this data provides proof-of-concept that a nano-cocktail is a viable strategy for combining molecular inhibitors. In addition, the lack of toxicity demonstrates the doses can be further modified to find the best strategy for not only arresting tumor growth, but inducing regression. The present study provides a rationale for utilizing nanoformulations as a means to realize the potential of combination therapy. Many combinations in the clinic have been plagued by overlapping side effects that require dose reduction or delay and lead to suboptimal dosing. The nano-cocktail nDCB:nTLZ however, demonstrate a potential to achieve a therapeutic response with a lower dose, potentially eliminating the suboptimal treatment brought on by dose reduction.

Abbreviations

CDK	Cyclin dependent kinase
CDKi	Cyclin dependent kinase inhibitor
PARP	Poly-(ADP-ribose) polymerase
PARPi	Poly-(ADP-ribose) polymerase inhibitor
HR	Homologous recombination
TNBC	Triple-negative breast cancer
<i>BRCA1/2</i>	Breast Cancer Gene 1/2
DSBs	Double strand breaks
DLS	Dynamic light scattering
DMSO	dimethylsulfoxide
PK	Pharmacokinetics
PBS	Phosphate buffered saline
PD	Pharmacodynamics
PLGA	Poly(lactic-co-glycolic) Acid
PEG	Polyethylene glycol
TEM	Transmission Electron Microscopy
HPLC	High Performance Liquid Chromatography
HGSOC	High grade serous ovarian cancer
H&E	Hematoxylin and eosin
i.v.	Intravenous
WBC	White blood cell
RBC	Red blood cell
PLT	Platelet
i.p.	Intraperitoneally
PDI	Polydispersity index
TLZ	Talazoparib
DCB	Dinaciclib
nTLZ	Nanoformulation of TLZ
nDCB	Nanoformulation of DCB
DCB[concentration]:TLZ[concentration]	Combination of certain concentrations of DCB and TLZ
nDCB[concentration]:nTLZ[concentration]	Combination of certain concentrations of nDCB and nTLZ
DCB[x]:TLZ[y]	Combination of certain ratio of DCB and TLZ;
nDCB[x]:nTLZ[y]	Combination of certain ratio of nDCB and nTLZ

Supplementary Information

The online version contains supplementary material available at <https://doi.org/10.1186/s12645-023-00240-4>.

Additional file 1: Figure S1. (A) Calculated IC_{50} of 3666 cell line. (B) Dose response curve of Free TLZ, nTLZ, and nTLZ with the addition of 25 nM nDCB for 4T1 cell line. Inhibitor vs. response curve and best fit IC_{50} values were generated

by GraphPad Version 9.5.1. *, $p < 0.05$, **, $p < 0.01$, ****, $p < 0.0001$. **Figure S2.** Individual tumor volume plots (A) and overall survival (B) of treatment groups compared to control. **Figure S3.** Change in body weight over time throughout the treatment period. Data only plotted if at least 50% of animals in the group were alive.

Acknowledgements

The authors would like to thank the Dana-Farber/Harvard Cancer Center for the use of the Rodent Histopathology Core.

Author contributions

Conception and design: PB, SS, SY; development of methodology: PB, SS, SY, NB; acquisition of data: PB, AO, SW, SY; analysis of data: PB, SY, NB; writing, review, and revision of manuscript: PB, SS, SY, NB. PB and SY contributed equally to this work. All authors reviewed the manuscript.

Funding

Open access funding provided by Northeastern University Library. This work was partially supported by W81XWH-16-1-0731 and HHS 5-R25-CA174650.

Availability of data and materials

The datasets used and/or analyzed during the current study are available from the corresponding author on reasonable request.

Declarations

Ethics approval and consent to participate

All animal studies were performed in accordance with protocol 17-1143R approved by the Institutional Animal Care and Use Committee at Northeastern University.

Consent for publication

Not applicable.

Competing interests

The nano-cocktail is the subject of intellectual property assigned to Northeastern University.

Received: 21 September 2023 Accepted: 12 December 2023

Published online: 23 March 2024

References

- Alagpulinsa DA, Ayyadevara S, Yaccoby S, Shmookler Reis RJ (2016) A cyclin-dependent kinase inhibitor, dinaciclib, impairs homologous recombination and sensitizes multiple myeloma cells to PARP inhibition. *Mol Cancer Ther* 15(2):241–250
- Baldwin P, Ohman AW, Medina JE, McCarthy ET, Dinulescu DM, Sridhar S (2019) Nanoformulation of Talazoparib delays tumor progression and ascites formation in a late stage cancer model. *Front Oncol* 9:353
- Bauer KR, Brown M, Cress RD, Parise CA, Caggiano V (2007) Descriptive analysis of estrogen receptor (ER)-negative, progesterone receptor (PR)-negative, and HER2-negative invasive breast cancer, the so-called triple-negative phenotype: a population-based study from the California cancer Registry. *Cancer* 109(9):1721–1728
- Bryant HE, Schultz N, Thomas HD, Parker KM, Flower D, Lopez E et al (2005) Specific killing of BRCA2-deficient tumours with inhibitors of poly(ADP-ribose) polymerase. *Nature* 434(7035):913–917
- Carey JPW, Karakas C, Bui T, Chen X, Vijayaraghavan S, Zhao Y et al (2018) Synthetic lethality of PARP inhibitors in combination with MYC blockade is independent of BRCA status in triple-negative breast cancer. *Cancer Res* 78(3):742–757
- Chou T-C, Martin N (2005) CompuSyn for drug combinations and for general dose-effect analysis. www.combosyn.com. 1–68
- Farmer H, McCabe N, Lord CJ, Tutt AN, Johnson DA, Richardson TB et al (2005) Targeting the DNA repair defect in BRCA mutant cells as a therapeutic strategy. *Nature* 434(7035):917–921
- Gonzalez-Angulo AM, Timms KM, Liu S, Chen H, Litton JK, Potter J et al (2011) Incidence and outcome of BRCA mutations in unselected patients with triple receptor-negative breast cancer. *Clin Cancer Res* 17(5):1082–1089
- Hartman AR, Kaldate RR, Sailer LM, Painter L, Grier CE, Endsley RR et al (2012) Prevalence of BRCA mutations in an unselected population of triple-negative breast cancer. *Cancer* 118(11):2787–2795
- Horiuchi D, Kusdra L, Huskey NE, Chandriani S, Lenburg ME, Gonzalez-Angulo AM et al (2012) MYC pathway activation in triple-negative breast cancer is synthetic lethal with CDK inhibition. *J Exp Med* 209(4):679–696
- Johnson N, Cai D, Kennedy RD, Pathania S, Arora M, Li YC et al (2009) Cdk1 participates in BRCA1-dependent S phase checkpoint control in response to DNA damage. *Mol Cell* 35(3):327–339
- Johnson N, Li YC, Walton ZE, Cheng KA, Li D, Rodig SJ et al (2011) Compromised CDK1 activity sensitizes BRCA-proficient cancers to PARP inhibition. *Nat Med* 17(7):875–882
- Johnson SF, Cruz C, Greifenberg AK, Dust S, Stover DG, Chi D et al (2016) CDK12 inhibition reverses de novo and acquired PARP inhibitor resistance in BRCA wild-type and mutated models of triple-negative breast cancer. *Cell Rep* 17(9):2367–2381
- Kulkarni S, Brownlie J, Jeyapalan JN, Mongan NP, Rakha EA, Madhusudan S (2022) Evolving DNA repair synthetic lethality targets in cancer. *Biosci Rep*. <https://doi.org/10.1042/BSR20221713>

- Lee A, Djamgoz MBA (2018) Triple negative breast cancer: emerging therapeutic modalities and novel combination therapies. *Cancer Treat Rev* 62:110–122
- Li Y, Zhang H, Merkher Y, Chen L, Liu N, Leonov S et al (2022) Recent advances in therapeutic strategies for triple-negative breast cancer. *J Hematol Oncol* 15(1):121
- Litton JK, Rugo HS, Ettl J, Hurvitz SA, Gonçalves A, Lee KH et al (2018) Talazoparib in patients with advanced breast cancer and a germline BRCA mutation. *N Engl J Med* 379(8):753–763
- Lord CJ, Ashworth A (2017) PARP inhibitors: synthetic lethality in the clinic. *Science* 355(6330):1152–1158
- Matulonis U (2018) Novel combination strategies for recurrent ovarian cancer. 12th Bienn Ovarian Cancer Res Symp. Seattle
- Mita MM, Joy AA, Mita A, Sankhala K, Jou YM, Zhang D et al (2014) Randomized phase II trial of the cyclin-dependent kinase inhibitor dinaciclib (MK-7965) versus capecitabine in patients with advanced breast cancer. *Clin Breast Cancer* 14(3):169–176
- Mita MM, Mita AC, Moseley JL, Poon J, Small KA, Jou YM et al (2017) Phase 1 safety, pharmacokinetic and pharmacodynamic study of the cyclin-dependent kinase inhibitor dinaciclib administered every three weeks in patients with advanced malignancies. *Br J Cancer* 117(9):1258–1268
- Murai J, Huang SY, Das BB, Renaud A, Zhang Y, Doroshow JH et al (2012) Trapping of PARP1 and PARP2 by Clinical PARP Inhibitors. *Cancer Res* 72(21):5588–5599
- Nemunaitis JJ, Small KA, Kirschmeier P, Zhang D, Zhu Y, Jou YM et al (2013) A first-in-human, phase 1, dose-escalation study of dinaciclib, a novel cyclin-dependent kinase inhibitor, administered weekly in subjects with advanced malignancies. *J Transl Med* 11:259
- Paige Baldwin SS, Bijay Singh, inventor; Northeastern University, assignee (2021) Nanoencapsulated combination drug formulations. United States patent 11648211. 25 Mar 2021
- Parry D, Guzi T, Shanahan F, Davis N, Prabhavalkar D, Wiswell D et al (2010) Dinaciclib (SCH 727965), a novel and potent cyclin-dependent kinase inhibitor. *Mol Cancer Ther* 9(8):2344–2353
- Shapiro GI, Do KT, Tolaney SM, Hilton JF, Cleary JM, Wolanski A et al (2017) Abstract CT047: Phase 1 dose-escalation study of the CDK inhibitor dinaciclib in combination with the PARP inhibitor veliparib in patients with advanced solid tumors. *Cancer Res* 77:CT047
- Singh B, Yang S, Krishna A, Sridhar S (2020) Nanoparticle formulations of poly (ADP-ribose) polymerase inhibitors for cancer therapy. *Front Chem* 8:594619
- Székely B, Silber AL, Pusztai L (2017) New therapeutic strategies for triple-negative breast cancer. *Oncology (williston Park)* 31(2):130–137
- Yang S, Wallach M, Krishna A, Kurmasheva R, Sridhar S (2021) Recent developments in nanomedicine for pediatric cancer. *J Clin Med* 10(7):1437
- Yang S, Green A, Brown N, Robinson A, Senat M, Testino B et al (2023) Sustained delivery of PARP inhibitor Talazoparib for the treatment of BRCA-deficient ovarian cancer. *Front Oncol* 13:1175617
- Zhang Y, Huo M, Zhou J, Xie S (2010) PKSolver: an add-in program for pharmacokinetic and pharmacodynamic data analysis in Microsoft Excel. *Comput Methods Programs Biomed* 99(3):306–314
- Zhang D, Baldwin P, Leal AS, Carapellucci S, Sridhar S, Liby KT (2019) A nano-liposome formulation of the PARP inhibitor Talazoparib enhances treatment efficacy and modulates immune cell populations in mammary tumors of BRCA-deficient mice. *Theranostics* 9(21):6224–6238

Publisher's Note

Springer Nature remains neutral with regard to jurisdictional claims in published maps and institutional affiliations.